

# Thermal, Optical, and Water Sorption Properties in Composite Films of Poly(ether imide) and Bismaleimides: Effect of Chemical Structure

Jongchul Seo,<sup>1</sup> Wonbong Jang,<sup>1</sup> Haksoo Han<sup>2</sup>

<sup>1</sup>Department of Packaging, Yonsei University, Wonju-si, Kangwondo, 220-710, Korea

<sup>2</sup>Department of Chemical Engineering, Yonsei University, 134 Seodaemun-Gu, Seoul, 120-749 Korea

Received 22 May 2007; accepted 23 August 2007

DOI 10.1002/app.29694

Published online 30 March 2009 in Wiley InterScience (www.interscience.wiley.com).

**ABSTRACT:** Two series of semi-interpenetrating polymer network (semi-IPN) composite films, PEI/bismaleimide (UTBM) and PEI/fluorinated BMI (UTFBM) were prepared using a thermoplastic PEI and two different crosslinkable imide moieties. The effects of chemical structure and content of crosslinkable imide moieties on thermal stability, dielectric properties, and water sorption have been investigated. Glass transition temperature and weight loss temperatures increased with increase in the content of crosslinkable imide moieties, indicating the enhanced thermal stability of the semi-IPN composite

films. The refractive indices of the semi-IPN composite systems increased with increasing crosslinkable imide moieties due to the higher polarizabilities of atoms. The water sorption of the semi-IPN composite films was significantly decreased by the incorporation of crosslinkable imide moieties, which are interpreted by morphological structure. © 2009 Wiley Periodicals, Inc. *J Appl Polym Sci* 113: 777–783, 2009

**Key words:** PEI; thermal stability; molecular order; water sorption; semi-IPN

## INTRODUCTION

Aromatic polyimides possess outstanding thermal, mechanical, and electrical properties as well as excellent chemical resistance.<sup>1–3</sup> Ultem 1000, a poly(ether imide) (PEI), has received significant attention from both academia and industry. It is an amorphous polymer offering high strength, excellent flame and heat resistance, and good melt processibility. There is no appreciable loss in mechanical properties up to 170°C, making it ideal for high strength/high heat applications, and those requiring consistent dielectric properties over a wide frequency range. PEI is commonly used for electrical/electronic insulators (including many semiconductor process components) and a variety of structural components requiring high strength and rigidity at elevated temperatures.

However, the monomeric unit of PEI contains two ether groups, four carboxylic groups, and two imide groups that are hydrophilic (see Fig. 1). In addition, these groups may hinder the order of interaction in polymer and lead to the amorphous and structureless morphological structure in PEI.<sup>4–6</sup> The high concentration of polar groups and poor morphological structure in PEI induced to relatively high water

sorption. The water sorption causes the potential reliability problems in microelectronic devices,<sup>1–3,5–10</sup> such as displacement, package crack, delamination, loss of adhesion, potential corrosion, and mechanical failures in thin films.

To reduce the water sorption in PEI, the semi-interpenetrating polymer network composite films were prepared from PEI and two different crosslinkable imide moieties, bismaleimide (BMI) and fluorinated bismaleimide (FBMI) (Fig. 1). The characteristic thermal, optical, and dielectric properties of the semi-IPN composite films have been investigated. Furthermore, the water sorption behaviors of the semi-IPN composite films have been gravimetrically investigated by using a thin film diffusion analyzer.<sup>8–12</sup> Thermal, optical, and water sorption properties of the semi-IPN composite films were correlated with the chemical structures of crosslinkable bismaleimide and different composition.

## EXPERIMENTAL

### Materials

The chemical structures of PEI and two crosslinkable imide moieties, bismaleimide (BMI) and fluorinated bismaleimide (FBMI), are shown in Figure 1. FBMI powder was synthesized from 4,4'-hexafluoroisopropylidene bis(phthalic anhydride) (6FDA), diaminodiphenylmethane (MDA), and maleic anhydride (MA) as a crosslink site.<sup>6</sup> BMI powder was purchased from

Correspondence to: H. Han (hshan@yonsei.ac.kr).

Contract grant sponsors: Ministry of Science and Technology, Korea (National Research Laboratory Program).

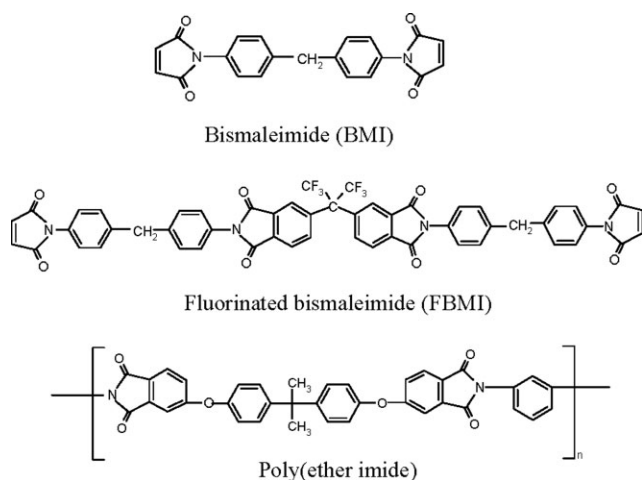


**Figure 1** Structures of the crosslinkable imide moieties and poly(ether imide).

Aldrich Chemical Co. General Electric supplied PEI (Ultem 1000), which is an amorphous thermoplastic with a number-average molar mass of  $20 \text{ kg mol}^{-1}$ , a density of 1.27, and a glass transition temperature ( $T_g$ ) of  $\sim 250^\circ\text{C}$ . PEI was dried under vacuum for 24 h at  $80^\circ\text{C}$  to remove moisture prior to use.

Various semi-IPN composites were prepared by dissolving the appropriate amounts of crosslinkable imide moieties and PEI in *N*-methyl-2-pyrrolidinone (NMP). The solid content of the polymer composite solution was about 10–15 wt %. Semi-IPN composite films were prepared by spin coating the polymer composite solution, followed by thermal treatment at  $300^\circ\text{C}$ . The ramping and cooling rates were 2.5 and  $2.0^\circ\text{C}/\text{min}$ , respectively. The thickness of the composite films was controlled in the range 10–13  $\mu\text{m}$  by a spin coator<sup>7–11</sup> and measured using a surface profiler (Tencor Instruments Co., Model AS500). Then, the cured films were detached from the substrates with the aid of deionized water, washed with distilled water several times, and dried under vacuum for 24 h.

The composite films thus obtained are designated on the basis of constituents and blend composition. For example, the composite films of PEI containing 0, 10, 25, and 40% (w/w) BMI are represented by UTBM0, UTBM10, UTBM25, and UTBM40, respectively. The letters UT and BM stand for PEI and BMI, respectively, and numerals represent the weight percent of BMI. Similarly, the semi-IPN composite films of PEI and FBMI are designated as UTFBM followed by numerals.

### Measurements

Fourier Transform infrared spectroscopy (FTIR, ATI Mattson Co., USA) analysis was performed to identify the crosslinking of BMI and FBMI in the range of  $400\text{--}4000 \text{ cm}^{-1}$ . Glass transition temperatures of

the semi-IPN composite films were determined by using a tensile head based dynamic mechanical thermal analyzer (DMTA, Polymer Laboratories, Model Mark III). The employed heating rate and frequency were  $5.0^\circ\text{C}/\text{min}$  and 1 Hz, respectively. Weight losses of the semi-IPN composite films were performed by a thermogravimetric analysis (TGA, TA Instruments), which were operated in nitrogen at a heating rate of  $10^\circ\text{C}/\text{min}$ .

The refractive indices of the semi-IPN composite films were measured by using a prism coupler (Metricon, Model 2010) with a He-Ne laser light of 632.8 nm wavelength. In the measurement, the resolution of refractive index was  $\pm 0.0005$ . A combination of TE and TM mode was used for measuring the in-plane and out-of-plane refractive indices. Dielectric constants at an optical frequency of 474.08 THz were calculated from the measured refractive indices using the Maxwell equation,  $\epsilon' = n^2$ .

For the morphology of the semi-IPN composite films, wide-angle X-ray diffraction (WAXD) patterns were obtained by using a wide angle goniometer (Rigaku Co., Model RINT 2500 H) with a monochromator (flat crystal type). The  $\text{CuK}\alpha$  radiation source ( $\lambda = 1.54 \text{ \AA}$ ) was operated at 40 kV and 40 mA and all the measurements were carried out at  $\theta/2\theta$  mode. Diffraction grams were collected over  $5\text{--}60^\circ$  ( $2\theta$ ) at  $0.02^\circ$  intervals with a scan speed of  $0.3\text{--}0.5^\circ \text{ min}^{-1}$ .

The water sorption behaviors of the semi-IPN composite films were gravimetrically investigated by using a thin film diffusion analyzer (CAHN Instruments Co., Model D-200). The water sorption isotherms were measured under  $25^\circ\text{C}$  and 100% relative humidity. The details are described in our previous studies.<sup>7–11</sup>

## RESULTS AND DISCUSSION

### FTIR analysis

The FTIR spectra of the UTBM and UTFBM semi-IPN composite films are shown in Figure 2. The characteristic imide bands are monitored around  $1780 \text{ cm}^{-1}$  (symmetric stretch of carbonyl groups),  $1720 \text{ cm}^{-1}$  (asymmetrical stretch of carbonyl groups),  $1370 \text{ cm}^{-1}$  (C-N stretch), and  $730 \text{ cm}^{-1}$  (deformation of imide ring). The crosslinking reaction of BMI and FBMI was monitored by the appearance of maleimide C=C band at  $1150 \text{ cm}^{-1}$ . The maleimide C=C at  $1150 \text{ cm}^{-1}$  disappeared after curing at  $300^\circ\text{C}$  for two semi-IPN composite films. BMI shows a polymerization onset temperature ( $T_i$ ) of the exothermic peak at  $180^\circ\text{C}$ , and a polymerization peak temperature of exothermic reaction around  $215^\circ\text{C}$ .<sup>13,14</sup> Considering the crosslinking process of BMI and FBMI, we selected  $300^\circ\text{C}$  as the curing temperature for the semi-IPN composite films, which indicates that BMI

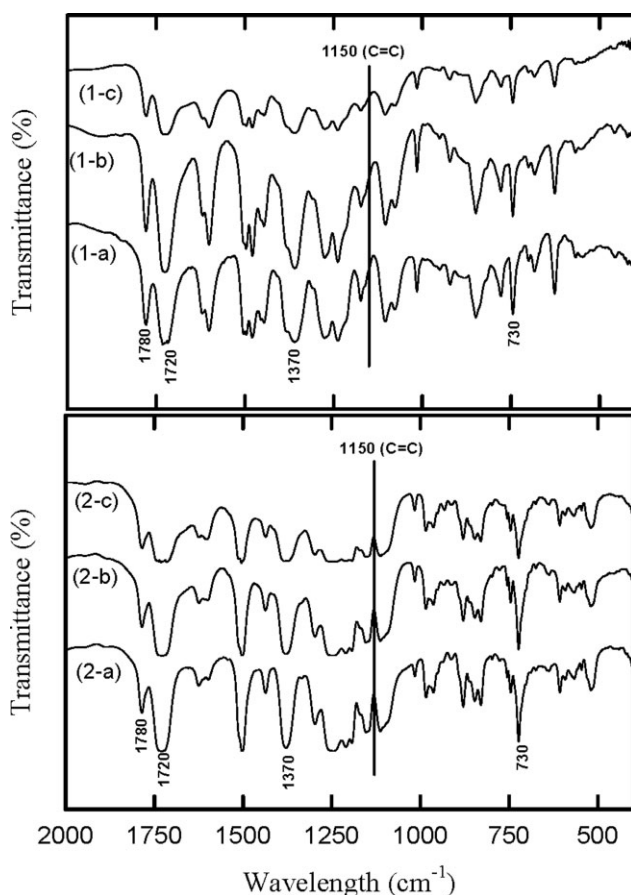


**Figure 2** FTIR spectra of the semi-IPN composite films: (1-a) UTBM0, (1-b) UTBM10, (1-c) UTBM40, (2-a) UTFBM0, (2-b) UTFBM10, and (2-c) UTFBM40.

and FBMI are fully reacted during the curing process.

### Thermal properties

To compare the thermal properties of the semi-IPN composite films,  $\tan \delta$  as a function of temperature are depicted in Figure 3. The single and symmetric damping peak-analogous to that observed in the neat PEI is detected for all the investigated composite films. In addition, its position shifts at higher temperature as the content of BMI and FBMI increases. These results indicate that the formation of a single and homogeneous system, at least up to the scale of the dynamic-mechanical test; that is, the phase domain, if it exists, is smaller than the size of the segments that are responsible for the primary molecular relaxation.<sup>15–17</sup> Figure 3 also shows the increase in the glass transition temperature of the composite films and decrease in mechanical loss with the crosslinkable moiety content. This is because with increase in crosslinking, the rigidity of the system increases and energy dissipation becomes difficult resulting in decrease in the  $\tan \delta$  values.

The  $T_g$  of the semi-IPN composites increased with increasing content of crosslinkable imide moieties for both of the two semi-IPN composite systems, which also indicate the enhancement of the rigidity in the system. With increase in the crosslinking the mobility of the polymer segments gets arrested resulting in high  $T_g$  of thermoplastic polymer PEI.

Figure 4 shows the TGA thermograms of the semi-IPN composite films and the 5 and 10% weight loss temperatures are summarized in Table I. The 5% weight loss temperatures ( $T_{5\text{wt}\%}$ ) increased from 522 to 563°C for the UTBM semi-IPN composite films, and from 522 to 539°C for the UTFBM semi-IPN composite films, respectively. From the TGA results, it can be concluded that the crosslinked structure can increase the thermal stability of the PEI as illustrated in the interpenetrating polymer network systems.<sup>18</sup> It may induce relatively high chain rigidity in crosslinkable moiety and increase in the degree of crosslinking, which may result in the enhanced thermal stability of the semi-IPN composite films. Specifically, the incorporation of BMI was more effective in the enhancement of thermal stability than that of FBMI. FBMI

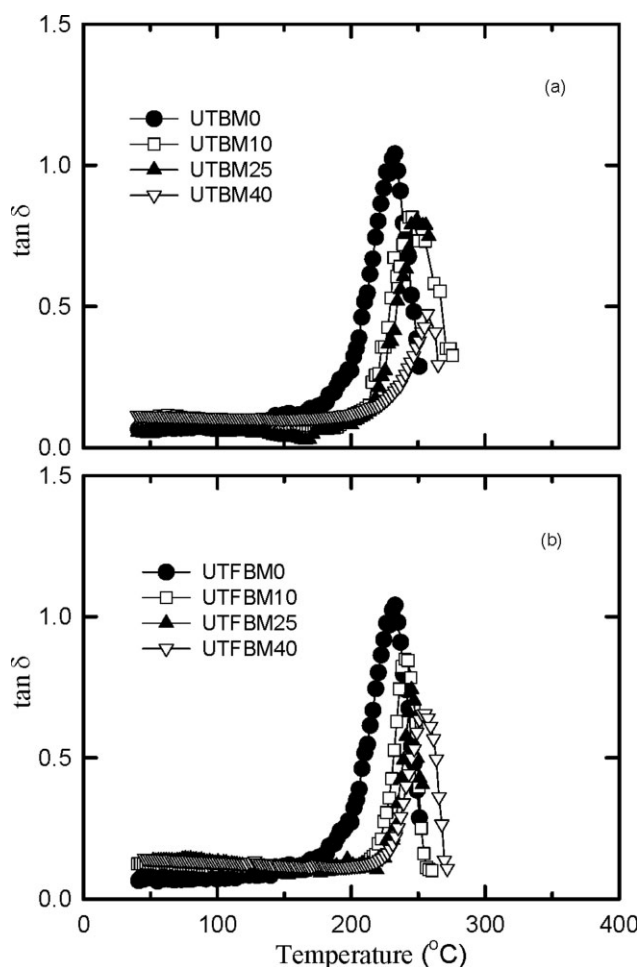


**Figure 3**  $\tan \delta$  as a function of temperature for the semi-IPN composite films; (a) UTBM and (b) UTFBM.

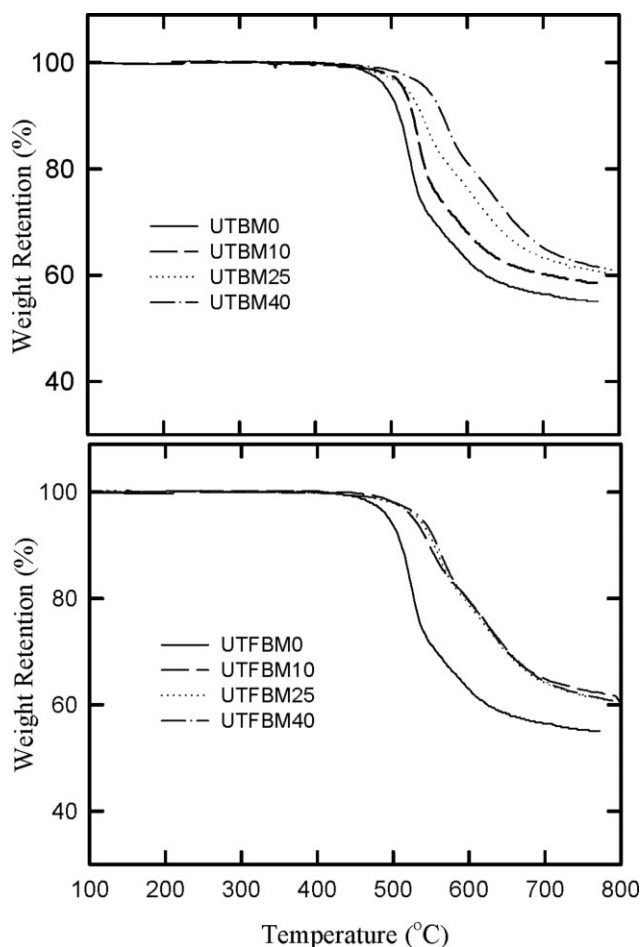


**Figure 4** TGA thermograms of the semi-IPN composite films under a nitrogen atmosphere.

contains flexible hexafluoroisopropylidene groups in the backbones, whereas BMI contains no flexible linkage in its backbone. Moreover, FBMI has a longer chain length than that of BMI. These factors can contribute toward higher rigidity of the resulting semi-IPN polymer network and consequently leading to

**TABLE I**  
Thermal Properties of the Semi-IPN Composite Films

Composites	Film thickness ( $\mu\text{m}$ )	Glass transition temperature ( $^{\circ}\text{C}$ )	Weight loss temperature	
			$T_{5\text{wt}\%}$ ( $^{\circ}\text{C}$ )	$T_{10\text{wt}\%}$ ( $^{\circ}\text{C}$ )
UTBM semi-IPN composite films				
UTBM0	12.52	230	522	538
UTBM10	11.11	245	540	552
UTBM25	11.42	249	555	567
UTBM40	10.98	255	563	575
UTFBM semi-IPN composite films				
UTFBM0	12.52	232	522	538
UTFBM10	9.56	240	532	547
UTFBM25	10.13	244	541	555
UTFBM40	9.79	257	539	557

greater enhancement in the thermal stability of the UTBM semi-IPN composite films.

### Optical and dielectric properties

Refractive indices of the semi-IPN composite films are summarized in Table II and Figure 5. All the composite films showed larger  $n_{xy}$  than  $n_z$  regardless of the compositions of the composite films. This indicates that polymer chains are preferentially aligned in the film plane, resulting in positive birefringence ( $\Delta = n_{xy} - n_z$ ) in the composite films.<sup>1-3,7-10</sup> With an increase in the BMI and FBMI content, the  $n_{xy}$  increased, consequently leading to increases in the average refractive  $n_{av}$ . However, UTBM semi-IPN composite films exhibited increasing trend in birefringence with increasing content of BMI, whereas FBMI semi-IPN composite films did not.

These refractive indices can be attributed to the polarizabilities of atoms constituting the backbones of crosslinkable imide moiety and a decrease in the free volume of the composite films.<sup>1,19</sup> For UTBM

**TABLE II**  
Optical and Dielectric Properties of the Semi-IPN Composite Films

Composites	Film thickness ( $\mu\text{m}$ )	Optical properties				Dielectric constant ( $\epsilon'_{av}$ ) <sup>c</sup>
		$n_{xy}$	$n_z$	$n_{av}$ <sup>a</sup>	$\Delta$ <sup>b</sup>	
UTBM semi-IPN composite films						
UTBM0	12.52	1.6539	1.6498	1.6525	0.0041	2.73
UTBM10	9.56	1.6607	1.6563	1.6592	0.0044	2.75
UTBM25	10.13	1.6629	1.6569	1.6609	0.0060	2.76
UTBM40	9.79	1.6675	1.6562	1.6637	0.0113	2.77
UTFBM semi-IPN composite films						
UTFBM0	12.52	1.6539	1.6498	1.6525	0.0041	2.73
UTFBM10	9.56	1.6557	1.6472	1.6529	0.0081	2.73
UTFBM25	10.13	1.6568	1.6528	1.6555	0.0040	2.74
UTFBM40	9.79	1.6573	1.6571	1.6572	0.0002	2.75

$$^a n_{av} = (2n_{xy} + n_z)/3.$$

$$^b \Delta = n_{xy} - n_z.$$

$$^c \epsilon'_{av} = (n_{av})^2.$$



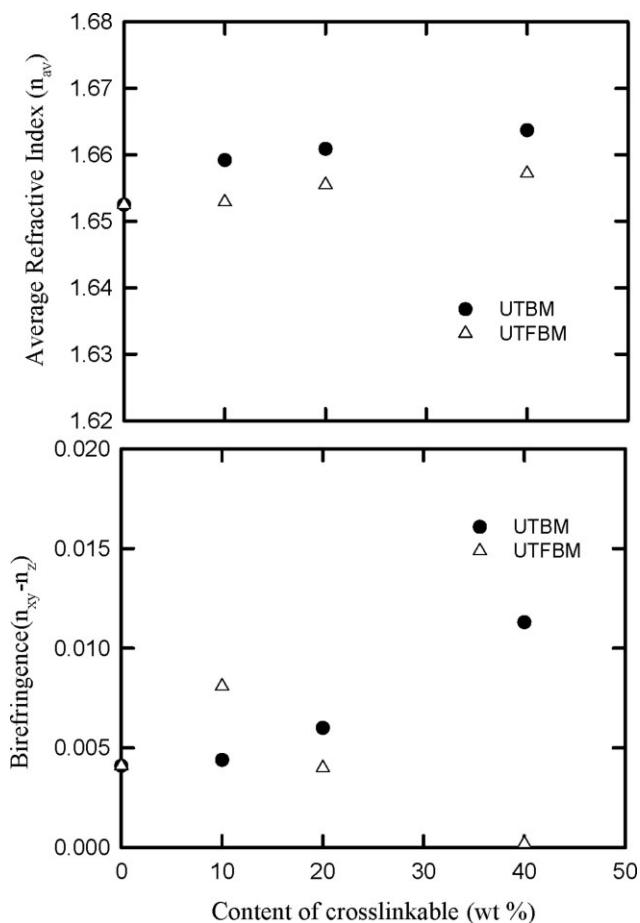


**Figure 5** Average refractive index and birefringence of the semi-IPN composite films.

semi-IPN composite films, the refractive index increased with the content of crosslinkable imide moieties. With increase in crosslinking, a compact structure was formed, which reduce the molar free volume, and also there is an increase in the number of polarizable atoms in a unit volume resulting in the increase in polarizability and refractive index.

Unlike BMI, FBMI crosslinkable moiety has fluorine atoms in one molecule. In general, higher polarizability causes a higher dipole moment under electromagnetic field, providing a higher refractive index. The fluorine atom exhibits a relatively low polarizability and low index of refraction, because of its high electronegativity.<sup>1,3,19</sup> Moreover, increases both in free volume due to bigger size of the  $CF_3$  groups and in interatomic repulsion of fluorine groups contribute to the decrease in the net polarizability of the system. These may explain the refractive index and birefringence of UTFBM semi-IPN composite films.

In general, the dielectric constant is proportional to the total polarization of the material including electronic, atomic, and dipolar polarizabilities. The dielectric constant equals the square of the refractive index

at an optical frequency according to the Maxwell relationship.<sup>1-3,19</sup> Dielectric constants of the semi-IPN composite films were calculated from the calculated average refractive indices, and they were given in Table II. With increase in the content of crosslinkable imide moieties, there is a small increment in dielectric constant, which varied in the range of 2.73–2.77 for the UTBM semi-IPN composite film, and in the range of 2.73–2.75 for the UTFBM semi-IPN composite film, respectively. However, the difference was very small, and there was no significant change in the dielectric constant of the semi-IPN composite films with increase in the content of crosslinkable imide moieties.

### Water sorption

The water sorption behaviors of the semi-IPN composite films were gravimetrically investigated at 25°C and 100% relative humidity, as shown in Figure 6. Water sorption isotherms of the semi-IPN composite films apparently followed the Fickian diffusion model well despite the morphological heterogeneities due to

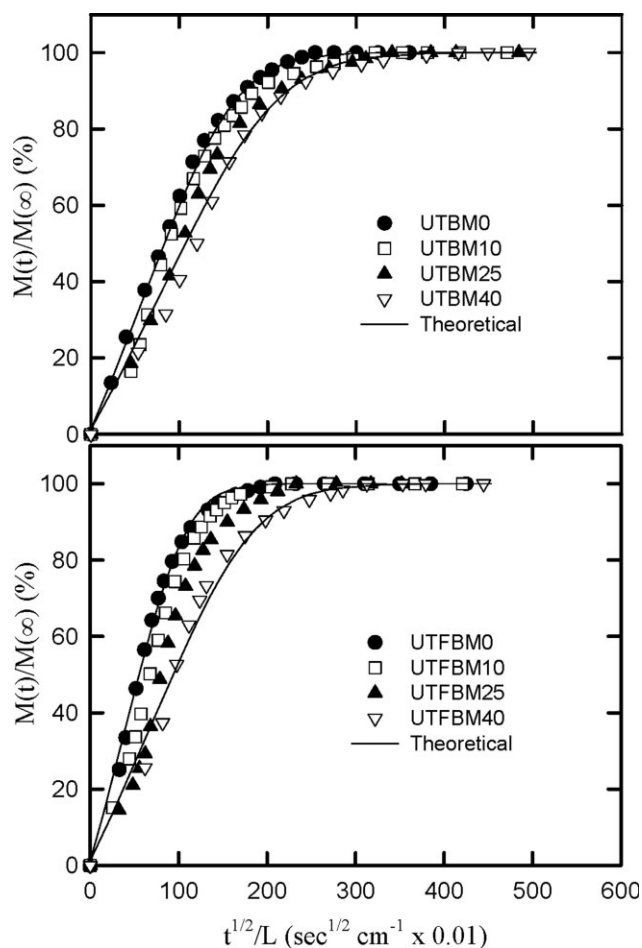


**Figure 6** Water sorption isotherms of the semi-IPN composite films.

**TABLE III**  
Water Uptakes and Diffusion Coefficients of the Semi-IPN Composite Films

Composites	Film thickness ( $\mu\text{m}$ )	Diffusion coefficient $D \times 10^{-10}$ ( $\text{cm}^2/\text{sec}$ )	Water uptake (wt %)
UTBM Semi-IPN composite films			
UTBM0	12.52	12.8	4.60
UTBM10	11.11	12.6	4.06
UTBM25	11.42	12.0	3.76
UTBM40	10.98	11.9	3.14
UTFBM semi-IPN composite films			
UTFBM0	12.52	12.8	4.60
UTFBM10	9.56	9.5	4.35
UTFBM25	10.13	8.4	4.23
UTFBM40	9.79	7.8	3.98

the ordered and disordered phases. Thus, all the water sorption isotherms were analyzed with the following equation, which is the mathematical solution for the water diffusion in an infinite slab with a constant surface concentration by Crank and Park<sup>20</sup>:

$$\frac{M(t)}{M(\infty)} = 1 - \frac{8}{\pi^2} \sum_{m=0}^{\infty} \frac{1}{(2m+1)^2} \exp\left(\frac{-D(2m+1)^2\pi^2 t}{L^2}\right) \quad (1)$$

where  $M(t)$  is the water sorption at a time  $t$ ,  $M(\infty)$  the water sorption at an infinite time ( $t = \infty$ ),  $D$  ( $\text{cm}^2/\text{s}$ ) the mutual diffusion coefficient of water and polymer system, and  $L$  is the film thickness. The experimental data of the entire range were fitted with eq. (1), leading to the estimation of the diffusion coefficient and water uptake of the semi-IPN composite films. The results are summarized in Table III.

The curves for the water diffusion coefficient and water uptake versus composition are shown in Figure 7. Both the diffusion coefficient and water uptake of the semi-IPN composite films decreased with increasing crosslinkable imide moieties regardless of imide moiety structure. It indicates that the water resistance capacity of PEI was greatly enhanced by the semi-IPN composite systems.

Usually, the water sorption behaviors of polymer films are correlated to the chemical structure and/or morphological structure.<sup>7,9-11</sup> PEI contains hydrophilic and flexible ether linkage in its backbone, which also induces amorphous nature and poor molecular ordering. The hydrophilic group and amorphous morphological structure of PEI may induce relatively high water uptake and diffusion coefficient. But the semi-IPN of PEI, which has a crosslinked network, which restricts the swelling of the PEI in water. Also, with increase in crosslinking, the water diffusion through the polyimide also got

reduced because of the formation of compact structure. Also, FBMI and BMI imide moieties have rigid structure, which induces to the more molecular ordering in the semi-IPN composite films which is also in conformance with the WAXD results.

The WAXD results are shown in Figure 8. Although both WAXD patterns had only one diffuse and amorphous halo, its intensity and sharpness increased with increasing the crosslinkable imide moieties. These WAXD results indicate that, though the semi-IPN composite films are structure-less, the molecular ordering increased with increasing content of FBMI and BMI imide moieties. In addition to the increase in the intensity of amorphous halo of the semi-IPN composite films, the UTBM composite films showed a slight indication, at an angle of  $4-8^\circ$ , that the intramolecular ordering in polymer chain increases.<sup>10,11,21</sup> These WAXD results showed good agreements with refractive index results shown in Table II. With increase in the content of crosslinkable imide moieties, the average refractive indices increased, indicating the increasing order in polymer chains.

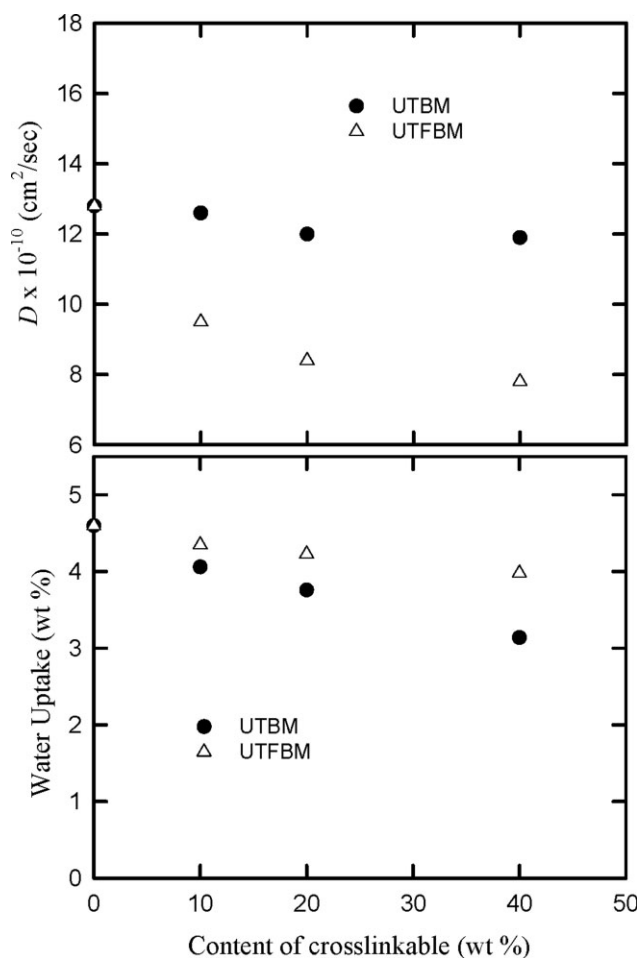


**Figure 7** Diffusion coefficients and water uptakes of the semi-IPN composite films.

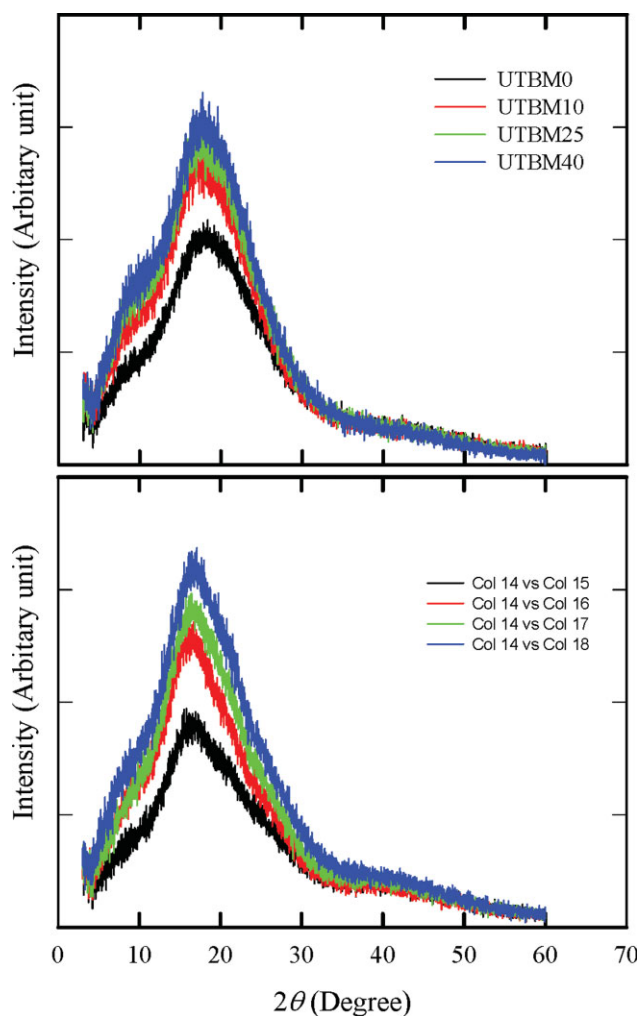


**Figure 8** WAXD patterns of the semi-IPN composite films. [Color figure can be viewed in the online issue, which is available at [www.interscience.wiley.com](http://www.interscience.wiley.com).]

## CONCLUSIONS

Two series of the semi-interpenetrating polymer network (semi-IPN) composite films, PEI/Bismaleimide (UTBM) and PEI/Fluorinated BMI (UTFBM), were prepared using thermoplastic PEI and two different crosslinkable imide moieties. The effects of type and content of crosslinkable imide moieties on thermal stability, optical, and water sorption properties of the semi-IPN composite films were investigated. Glass transition temperature and weight loss temperature increased with increase in the content of crosslinkable imide moieties, indicating the enhanced thermal stability of the semi-IPN composite films.

The refractive indices of the semi-IPN composite films increased with increasing crosslinkable imide moieties due to the higher polarizable atoms. The water sorption of the semi-IPN composite films was significantly decreased by incorporating the crosslinkable imide moieties, because of both reduction in polymer swelling and enhanced molecular order. In conclusion, incorporating BMI in PEI is more effective to increase the thermal stability and decrease the water sorption than FBMI with bulky and flexible interlinkage.

This work was supported by Korea Energy Management Corporation.

## References

1. Ghosh, M. K.; Mittal, K. L. *Polyimides: Fundamentals and Applications*; Marcel Dekker: New York, 1996.
2. Feger, C. *Polyimides: Trends in Materials and Applications*; Society of Plastics Engineers: New York, 1996.
3. Mittal, K. L. *Polyimides: Synthesis, Characterization, and Application*; Plenum Press: New York, 1996.
4. Merdas, I.; Thominet, F.; Verdu, J. *J Appl Polym Sci* 2000, 77, 1439.
5. Merdas, I.; Thominet, F.; Verdu, J. *J Appl Polym Sci* 2000, 77, 1445.
6. Srinivas, I.; Caputo, F. E.; Wilkes, G. L. *Macromolecules* 1997, 30, 1012.
7. Han, H.; Seo, J.; Ree, M.; Pyo, S. M.; Gryte, C. C. *Polymer* 1998, 39, 2963.
8. Seo, J.; Han, H.; Kim, S.; Chung, H.; Joe, Y. I. *Polym J* 1999, 31, 127.
9. Han, H.; Gryte, C. C.; Ree, M. *Polymer* 1995, 36, 1663.
10. Seo, J.; Han, C. S.; Han, H. *J Polym Sci Part B: Polym Phys* 2001, 39, 669.
11. Seo, J.; Lee, C.; Jang, W.; Sundar, S.; Han, H. *J Appl Polym Sci* 2006, 99, 1692.
12. Seo, J.; Jang, W.; Han, H. *Macromol Res* 2007, 15, 10.
13. Torrecilla, R.; Regnier, N.; Mortaigne, B. *Polym Degrad Stab* 1996, 51, 307.
14. Kurdi, J.; Kumar, A. *Polymer* 2007, 53, 301.
15. Musto, P.; Martusceli, E.; Ragosta, G.; Russo, P.; Scarinzi, G.; Villano, P. *J Mater Sci* 1998, 33, 4595.
16. Lu, G.; Huang, Y.; Yan, Y.; Zhao, T.; Yu, Y. *J Appl Polym Sci* 2006, 102, 76.
17. Woo, E. M.; Chen, L. B.; Seferis, J. C. *J Mater Sci* 1987, 22, 3665.
18. Sperling, L. H. *Interpenetrating Polymer Networks and Related Materials*, Plenum Press, New York, 1981.
19. Van Krevelen, D. W. *Properties of Polymers*; Elsevier: Amsterdam, 1990.
20. Crank, J.; Park, G. S. *Diffusion in Polymers*; Academic Press: London, 1968.
21. Van Alsten, J. G.; Coburn, J. C. *Macromolecules* 1994, 27, 3746.